International Journal of Pharmaceutics 388 (2010) 242–250

Contents lists available at ScienceDirect

International Journal of Pharmaceutics

journal homepage: www.elsevier.com/locate/ijpharm

Pharmaceutical nanotechnology

Silk fibroin nanoparticles for cellular uptake and control release

Joydip Kundu [a], Yong-Il Chung [b], Young Ha Kim [b], Giyoong Tae [b,*], S.C. Kundu [a,**]

[a] Department of Biotechnology, Indian Institute of Technology, Kharagpur 721302, West Bengal, India
[b] Department of Nanobio Materials and Electronics and Department of Material Science and Engineering, Gwangju Institute of Science and Technology, 261 Cheomdan-gwagiro (Oryong-dong), Buk-gu, Gwangju, 500-712, Republic of Korea

ARTICLE INFO

Article history:
Received 20 August 2009
Received in revised form
20 December 2009
Accepted 24 December 2009
Available online 8 January 2010

Keywords:
Silk fibroin
Nanoparticles
Biomaterials
TEM
Cellular uptake
VEGF

ABSTRACT

Silk nanoparticles were prepared from silk fibroin solutions of domesticated *Bombyx mori* and tropical tasar silkworm *Antheraea mylitta* and investigated in respect to its particle size, surface charge, stability and morphology along with its cellular uptake and release of growth factors. The nanoparticles were stable, spherical, negatively charged, 150–170 nm in average diameter and exhibited mostly Silk II (β-sheet) structure and did not impose any overt toxicity. Cellular uptake studies showed the accumulation of fluorescence isothiocyanate conjugated silk nanoparticles in the cytosol of murine squamous cell carcinoma cells. *In vitro* VEGF release from the nanoparticles showed a significantly sustained release over 3 weeks, signifying the potential application as a growth factor delivery system.

1. Introduction

The promising significance of nanoparticles in the biomedical fields and the severe needs of materials with biocompatibility, biodegradability, and non-toxicity have propelled the efforts for developing and optimizing new materials. Various types of polymeric nanoparticles like solid lipid particles (Muller et al., 2000), micelles (Torchilin, 2004), liposomes (Cheema et al., 2007), and dendrimers (Svenson and Tomalia, 2005) have been reported as nanodelivery systems to encapsulate the drugs and other biotechnology products such as growth factors and genes (Azarmi et al., 2006; Liu et al., 2007). Biodegradable nanoparticles can be produced from natural or synthetic macromolecules like serum albumin, gelatin, polycyanoacrylates, polylactic-co-glycolic acid, and chitosan (Le et al., 1999; Chung et al., 2006; Kocbek et al., 2007; Won and Kim, 2008). Protein based nanoparticles generally vary in size from 50 to 300 nm (Azarmi et al., 2006) and they hold certain advantages such as greater stability during storage, stability in vivo, non-toxic, non-antigenic (Soppimath et al., 2002) and ease to scale up during manufacture (Balthasar et al., 2005) over the other drug delivery systems.

Silk fibroin protein obtained from mulberry silkworms of *Bombyx mori* is a protein based biomacromolecule composed of 5507 amino acid repeats consisting of repeated sequences of six residues of $(Gly\text{-}Ala\text{-}Gly\text{-}Ala\text{-}Gly\text{-}Ser)_n$ repeats. Biopolymer is a heterodimeric protein with a heavy chain (395 kDa) and a light chain (25 kDa) which are linked by a single disulfide bond (Inoue et al., 2000) at cys-172 of the L-chain and cys c-20 (twentieth residue from c terminus) of H chain (Tanaka et al., 1999). The silk fibroin protein of non-mulberry tropical tasar silkworm *Antheraea mylitta* is a homodimeric protein of 395 kDa and, with each monomer approximately 197 kDa (Datta et al., 2001). The silk fibroin protein is used as biomaterials in the form of films (Kundu et al., 2008a,b) three-dimensional scaffolds (Nazarov et al., 2004), hydrogels (Kim et al., 2004) electrospun fibers (Jin et al., 2002) and microspheres (Wang et al., 2007). Recently, silk gland fibroin isolated from tropical tasar silkworm *A. mylitta* has been utilized as a promising biomaterial for tissue engineering (Mandal and Kundu, 2008). Silk fibroin protein powder has been used as an additive to cosmetics, food, and as biomaterials due to its excellent properties like moisture absorption and considerate likeness to human skin (Xu et al., 2006).

Studies on protein based nanoparticles as a vehicle for drug delivery systems have centered mainly on the albumin and gelatin nanoparticles (Kaul and Amiji, 2005; Kommareddy and Amiji, 2005; Xu et al., 2006). Generally three different methods are utilized for the fabrication of protein based nanoparticles namely, emulsion formation, coacervation or desolvation, water-in-oil emulsion

* Corresponding author. Tel.: +82 62 970 2305; fax: +82 62 970 2304.
** Corresponding author. Tel.: +91 3222 283764; fax: +91 3222 278433.
E-mail addresses: gytae@gist.ac.kr (G. Tae), kundu@hijli.iitkgp.ernet.in (S.C. Kundu).

0378-5173/$ – see front matter © 2010 Elsevier B.V. All rights reserved.
doi:10.1016/j.ijpharm.2009.12.052

(Weber et al., 2000). Like other natural proteins (Balthasar et al., 2005; MaHam et al., 2009) fibroin has been exploited as a drug carrier system owing to its chemical and physical nature (Hofmann et al., 2006; Uebersax et al., 2007). The influence of pH and temperature on the phase behavior of fibroin in solution makes it an interesting candidate for drug delivery applications (Liu et al., 2009). The abundant functional groups offer the advantage of incorporating more functionalities and modifications via chemical derivatization.

This study reports the fabrication of silk protein fibroin spherical nanoparticles from both mulberry and non-mulberry silk utilizing dimethyl sulfoxide as desolvating agent. The investigation outlines the formation of nanoparticles, their morphology, surface properties, conjugation with fluorescence isothiocyanate and the cellular uptake of these nanoparticles by murine squamous cell carcinoma as well as VEGF release from the nanoparticles to explore their use as potential therapeutic drug delivery system.

2. Experimental

2.1. Materials and methods

Fresh cocoons of *B. mori* silkworm were collected from the Debra Sericulture farm, West Midnapore, West Bengal and non-mulberry 5th instar mature live larvae of *A. mylitta* were collected from Jhargram sericulture farm, Midnapore, India. Sodium dodecyl sulfate (J T Baker, Phillipsburg, NJ, USA), dimethyl sulfoxide (Sigma–Aldrich), lithium bromide (Sigma–Aldrich), cellulose tubing of cut off 12,000 (Pierce, USA), thiazolyl blue (MTT, Sigma, USA) Cell culture grade chemicals such as Dulbecco's modified Eagle's medium (DMEM), fetal calf serum, trypsin and penicillin, streptomycin antibiotics (Gibco BRL, USA) and other chemicals purchased from Sigma or Aldrich were used without further purification.

2.2. Preparation of silk fibroin solution from Bombyx mori cocoon

Silk fibroin protein was isolated from cocoons of *B. mori* following standard extraction procedure (Jin et al., 2005) with slight modification. Briefly, cocoons were cut into small pieces, boiled with 0.02 (M) Na_2CO_3 for 60 min and washed with milli-Q water several times to remove sericin from the silk fibers and the degummed fibers were then dried completely. The degummed fibers were dissolved in 9.3 (M) LiBr at 60 °C for 4 h. The regenerated silk fibroin solution was then dialyzed in cellulose tube (12 kDa, MWCO) against deionized water for 48 h with several changes to remove the residual lithium bromide. Fibroin solution was then collected and the concentration was determined by weighing the remaining solid after drying the solution at 60 °C.

2.3. Isolation of silk fibroin protein solution from Antheraea mylitta silk gland

Silk fibroin protein was isolated from the posterior silk glands of mature 5th instar larvae of non-mulberry tropical tasar silkworm, *A. mylitta* following the isolation procedure as reported earlier (Mandal and Kundu, 2008). In brief, silk gland was placed in phosphate buffer (pH 7.4) for removal of sericin which binds the fibroin. The glands were squeezed with fine forceps to separate fibroin from gland membrane and extrude the protein. The silk fibroin isolated from silk gland was either used immediately or was stored at −20 °C in eppendorf tubes till further use. The frozen silk gland protein was thawed at room temperature and dissolved in 1% SDS (sodium dodecyl sulfate) aqueous solution containing 10 mM Tris (pH 8.0) and 5 mM EDTA at room temperature for 1 h. The regenerated silk fibroin solution was dialyzed in a cellulose tube (12 kDa, MWCO) against deionized water for 24 h with several changes to remove residual SDS (Mandal and Kundu, 2008). Fibroin solution was then collected and the concentration was determined by weighing the remaining solid after drying the solution at 60 °C similar to that mentioned earlier.

2.4. Fabrication of silk fibroin protein nanoparticles

Desolvation technique were implemented for the preparation silk protein fibroin nanoparticles (Weber et al., 2000) using dimethyl sulfoxide (DMSO) as desolvating agent. In brief, the fabrication process consisted of the following steps namely, protein isolation, desolvation, centrifugation, purification, sonication, filtration and lyophilization. To induce the desolvation process, 10 ml of anhydrous DMSO was taken in a small glass bottle/container and 10 ml of regenerated silk fibroin solution (2%, w/v) was added drop wise (50 μl/drop) at room temperature with constant stirring at a very low rpm. After desolvation, the formations of the silk nanoaggregates (nanoparticles) were visible in the form of precipitates produced at the bottom. Silk fibroin nanoaggregates (nanoparticles) were then centrifuged twice at 23,500 × *g* for 10 min to collect the precipitates. Silk fibroin precipitates were then further purified with repeated centrifugation at 13,400 × *g* for 10 min in deionized water. The purified nanoparticles pellet was then redispersed in deionized water by sonication at 30% amplitude for 20 min (pulse of 5 min ON and 5 min OFF) to get the protein/silk nanoparticle suspension in deionized water to remove the DMSO. The nanoparticles were filtered through a 0.45 μm syringe filter to remove dust particles/contaminants. The filtered nanoparticle suspension was lyophilized to get the freeze-dried nanoparticles and the resultant nanoparticles are stored at 2–8 °C.

2.5. Preparation of FITC labeled silk fibroin protein nanoparticles

Synthesis of FITC (fluorescein isothiocyanate) labeled fibroin nanoparticles was based on the isothiocyanate group of the FITC and the primary amino group of the silk fibroin (Zhao and Wu, 2006) Briefly, 100 mg of FITC in 10 ml of DMSO was slowly added to 10 ml of 1 mg/ml silk fibroin nanoparticles suspension. The reaction between the isothiocyanate group of FITC and the amino group of the protein was allowed to proceed for 10 h in the dark at room temperature. FITC labeled fibroin nanoparticles were then precipitated by raising the pH to 8–9 with 0.5 M NaOH. To remove the unconjugated FITC, the precipitate was subjected to repeated cycles of washing and centrifugation (13,400 × *g* for 10 min) until no fluorescence was detected in the supernatant (RF-5301 spectrofluorophotometer, λ_{exe} 490 nm, λ_{emi} 520 nm). The FITC conjugated nanoparticle was then dialyzed in a cellulose tube (12 kDa, MWCO) for 3 days in the dark against 5 l of distilled water, the water replaced on a daily basis.

2.6. Nanoparticle size and surface potential

Nanoparticle size and size distribution were determined by laser light scattering with particle size analyzer (ELS-8000, Electrophoretic Light scattering unit, Photal, Otsuka Electronics) at a fixed angle of 90° at 25 °C. Briefly, the dried silk fibroin nanoparticles were suspended in filtered deionized water and sonicated (30% amplitude for 20 min, pulse of 5 min ON and 5 min OFF) to obtain uniform dispersion of the nanoparticles. The dispersity of the particles is calculated by determining the polydispersity index. The higher the polydispersity, larger is the polydispersity index and hereby higher is the particle size variation. The data represent the average values of five measurements with accumulation times of 300. The surface charge (zeta potential) of the nanoparticle was also measured using the same equipment at 25 °C ($n = 3$) in deionized

Table 1
Particle size, polydispersity index and surface charge of silk fibroin nanoparticles fabricated from regenerated fibroin protein solution obtained from *Antheraea mylitta* silk gland and *Bombyx mori* cocoon fibroins. The nanoparticles are dispensed in water and in cell culture medium.

Nanoparticles fabricated from	Dispersing medium	Diameter[a] (nm)	Polydispersity[b]	Zeta potential[c] (mV)
A. mylitta	Deionized water	157 ± 4	0.020	−26.15
A. mylitta	DMEM[d] (10% FBS[e])	168 ± 1	0.023	−5.06
B. mori	Deionized water	177 ± 3	0.027	−24.41
B. mori	DMEM (10% FBS)	179 ± 2	0.028	−5.21

[a] Average ± standard deviation ($n = 5$) and accumulation times = 300.
[b] Average value.
[c] Average of three values are given in the table ($n = 3$).
[d] Dulbecco's modified Eagle's medium.
[e] Fetal bovine serum.

water and also in water containing 10% (v/v) fetal bovine serum (FBS, Hyclone) at a pH around 7.

2.7. Stability of nanoparticles

The stability of the nanoparticles was determined by monitoring their mean particle size in deionized water and fetal bovine serum (FBS) containing deionized water using laser light scattering with particle size analyzer at a fixed angle of 90° at 25 °C. After production, the nanoparticles were incubated at 37 °C in the incubator and their sizes were determined after 1, 4, 24, 25, 48, 72, 96, and 168 h, respectively.

2.8. Fourier Transform infrared spectroscopy (FT-IR)

The FT-IR spectra of the lyophilized silk fibroin nanoparticles were obtained using PerkinElmer FT-IR spectrophotometer (Spectrum GX). The IR spectra in absorbance mode were obtained in the spectral regions of 800–2000 cm^{-1}. The spectrum of each sample was acquired by accumulation of 3 scans with a resolution of 4 cm.

2.9. X-ray diffraction (XRD)

Wide-angle XRD patterns of the silk protein fibroin nanoparticles prepared from both *B. mori* and *A. mylitta* were measured by an X-ray diffractometer (PANalytical, X'Pert PRO PW3040/60) using Cu Kα radiation (λ = 1.54 Å) in the 2θ range of 100–400 at 40 kV, 30 mA.

2.10. High resolution transmission electron microscopy (HRTEM)

Information on the morphology of the silk fibroin nanoparticles was obtained by using a transmission electron microscope. TEM samples were prepared by dropping 20 μl of nanoparticles dispersion in deionized water on carbon coated electron microscopy grids. The specimens were air dried in dust free condition before examination under JEOL JEM-2100 transmission electron microscope (voltage applied: 200 kV).

2.11. Cell culture

Murine fibroblasts cell line L929 (National Center for Cell Sciences, NCCS, Pune) were chosen for cell culture studies, as these fibroblasts were highly stable, fast growing and represent well defined internal cytoskeleton components. The fibroblasts were seeded onto a 24-well tissue culture plate at a density of 1×10^4 cells per well for 24 h after which the growth medium was removed and replaced with the medium containing silk protein fibroin nanoparticles. For control experiments, medium without nanoparticles was used. The medium used was 90% Dulbecco's modified Eagle's medium (DMEM), 9.0% fetal calf serum (FBS) (Hyclone), 1.0% 200 mM L-glutamine, and 0.9 wt% 100 mM sodium pyruvate.

2.12. Cell viability/cytotoxicity studies

The MTT (3-(4,5-dimethylthiazol-2-yl)-2,5-diphenyltetrazolium bromide) assay was used to measure the cell cytotoxicity. The L929 murine fibroblast cells were plated at a density of 1×10^4 cells/well in 96-well plates at 37 °C in 5% CO_2 atmosphere. After 24 h of culture, the medium in the well was replaced with fresh medium containing nanoparticles of varying concentrations. Silk protein fibroin nanoparticles prepared from non-mulberry tasar silkworm *A. myliita* was used for determination of biocompatibility of the silk nanoparticles. After 24 h, 20 μl of MTT dye solution (5 mg/ml in phosphate buffer at pH 7.4, MTT Sigma) was added to each well. After 4 h of incubation at 37 °C and 5% CO_2 for exponentially growing cells and 15 min for steady-state confluent cells, the medium was removed and formazan crystals were solubilized with 200 μl of DMSO and the solution was vigorously mixed to dissolve the reacted dye. The absorbance of each well was read on a microplate reader at 570 nm.

2.13. Flow cytometric analysis

L929 murine fibroblast cells were seeded at a density of 1×10^6 cells/well and incubated with silk protein fibroin nanoparticles (100, 250 and 500 μg/ml) placed within the 6-well plates. The wells without the nanoparticles were taken as the control. The seeded

Table 2
Determination of stability of silk fibroin protein nanoparticles prepared with the silk protein isolated from *A. mylitta* using the particle size analyzer in deionized water and serum containing media ($n = 5$ and accumulation times = 300).

Time	Deionized water		Serum containing media	
	Diameter (nm)	Polydispersity	Diameter (nm)	Polydispersity
1 h	157 ± 4	0.020	168 ± 1	0.023
4 h	155 ± 4	0.024	180 ± 3	0.025
24 h	159 ± 4	0.023	190 ± 2	0.021
25 h	159 ± 4	0.023	197 ± 5	0.019
48 h	155 ± 3	0.022	199 ± 1	0.023
72 h	154 ± 2	0.022	196 ± 2	0.024
96 h	153 ± 4	0.022	191 ± 2	0.020
168 h	155 ± 3	0.021	192 ± 1	0.023

cells were incubated for 24 h with/without nanoparticles. After the desired incubation time, the cells were harvested by addition of 2 ml of 0.25% trypsin–EDTA to the samples. They were then incubated at 37 °C in an incubator until all cells were detached from the flask. The trypsinized cell suspension was neutralized with 5 ml complete medium, followed by centrifugation at 201 × *g* for 10 min. Cell pellet was suspended in cold PBS and centrifuged for 10 min at 1000 rpm. To the cell pellet 70% chilled ethanol was added in shaking condition and incubated at 4 °C for 45 min followed by washing with PBS twice. The cell pellet was resuspended in 200 μl PBS containing 0.1 mg/ml RNase and incubated for 30 min at 37 °C. The pellet was further washed in PBS. The samples were centrifuged and resuspended in 0.5 ml PBS containing 20 μl of PI solution (1 mg/ml PI). After another 30 min of incubation in the dark at 4 °C, the resultant cell suspension was analyzed with a flow cytometer (FACS Calibur, BD using Cell Quest Pro software) at 488 nm excitation and a 560 nm band pass filter for red fluorescence of propidium iodide.

2.14. Cellular uptake of the nanoparticles

Murine squamous cell carcinoma line (SCC7) was used for the cell uptake studies. SCC7 cells were cultured in medium (RPMI 1640; GIBCO 11875) containing 10% fetal bovine serum (GIBCO 16000-044), 2 mmol/l glutamine, and a mixture of 50 IU/ml penicillin and 50 g/ml streptomycin (GIBCO 15140-122) at 37 °C with 5% CO_2 in a CO_2 incubator (NUAIRE). After initial passage in culture petri dish (100 mm × 20 mm, polystyrene treated, Corning Incorporated, Corning International) murine squamous cell carcinoma line (SCC7) was grown to semi-confluence in medium containing 10% serum, 2 mmol/l glutamine, and a mixture of 50 IU/ml penicillin and 50 g/ml streptomycin in 24-well tissue culture plates on corning circular glass cover slips at 37 °C with 5% CO_2 atmosphere in a CO_2 incubator. After filtration, the nanoparticle suspension (200 μg/ml) was incubated with cells at 37 °C, 5% CO_2 atmosphere for a period of 30, 60, 120 and 360 min, respectively. After final wash with PBS, the cells were fixed with 4% (v/v) paraformaldehyde in PBS for 30 min at room temperature and washed four times with sterile PBS. Individual cover slips were then mounted with the cell side up on clean glass slides with fluorescence free glycerol based mounting medium and images were acquired with a confocal microscope (Olympus FV1000).

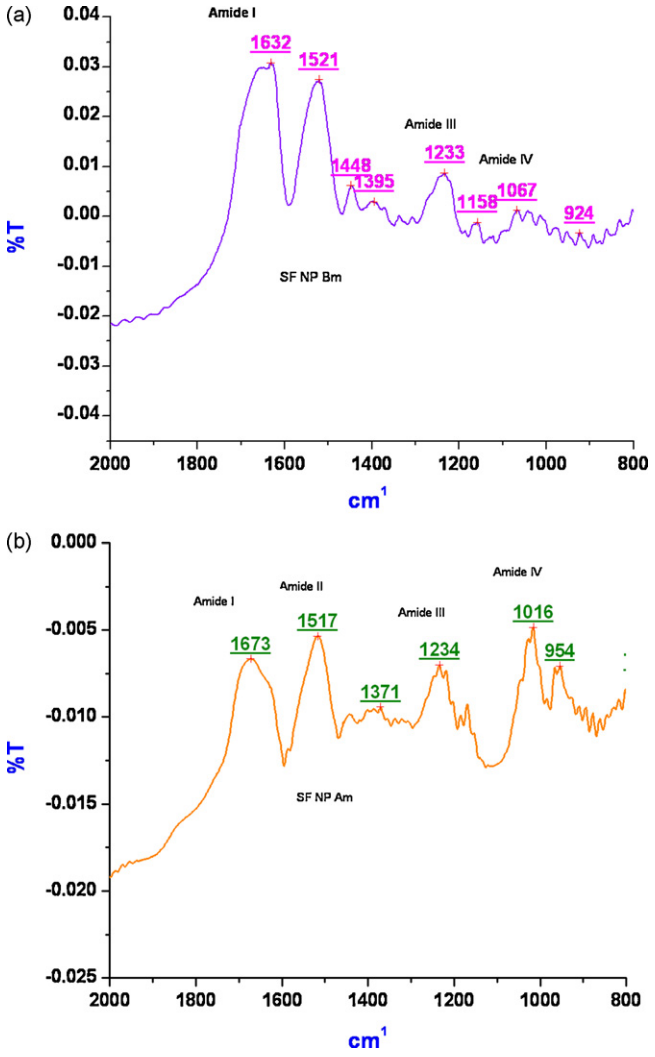

Fig. 1. FT-IR spectra of silk fibroin protein nanoparticles of (a) *Bombyx mori* (SFNP Bm) and (b) *Antheraea mylitta* (SFNP Am) using PerkinElmer FT-IR spectrophotometer (scan range 800–2500 cm^{-1}).

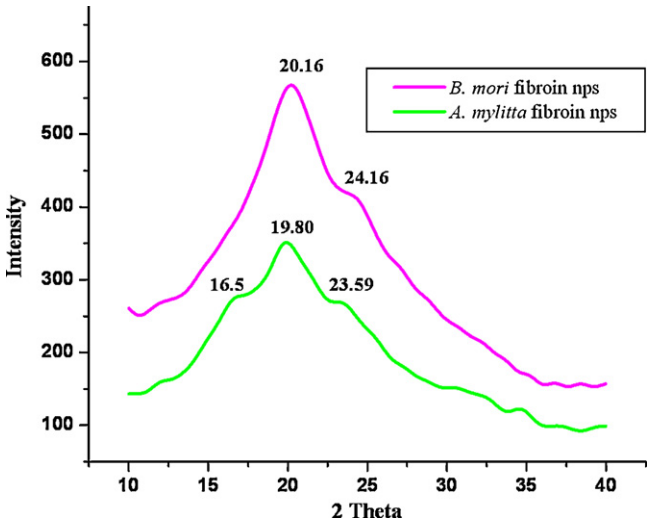

Fig. 2. X-ray diffraction of silk fibroin protein nanoparticles of *B. mori* and *A. mylitta* (SFNP Bm, SFNP Am) using X-ray diffractometer (PANalytical, X'Pert PRO PW3040/60) using Cu Kα radiation (λ = 1.54 Å) in the 2θ range of 10° to 40°.

2.15. In vitro vascular endothelial growth factor (VEGF) release

Silk protein fibroin nanoparticles prepared from non-mulberry tasar silkworm *A. myliita* was used for the vascular endothelial growth factor release from the nanoparticles. In brief, 200 μl silk protein fibroin nanoparticle suspensions (25 mg/ml) were mixed with 10 μl PBS containing 100 ng of rhVEGF (PeproTech, USA) and then incubated at 4 °C overnight with gentle stirring. Then, VEGF-loaded nanoparticle suspension was subsequently put into a 250 μl dialysis membrane tube (MWCO 300 K, Spectrum, USA) covering the open end of the tube. The tube was placed into 35 ml PBS with 2.0 mM sodium azide and 0.01% (w/v) BSA, and incubated at 37 °C with gentle shaking. As the control, the system without the silk nanoparticles containing 100 ng of VEGF was prepared. At pre-determined time intervals, aliquots (300 μl) of the release buffer were taken and stored at −70 °C until they were analyzed. To maintain a sink condition during the release experiment, 300 μl of fresh buffer was added to the release buffer after sampling, and the buffer was totally replaced with an equal volume of fresh buffer regularly. The released amount of total VEGF was characterized using the Human VEGF ELISA kit (PeproTech, USA).

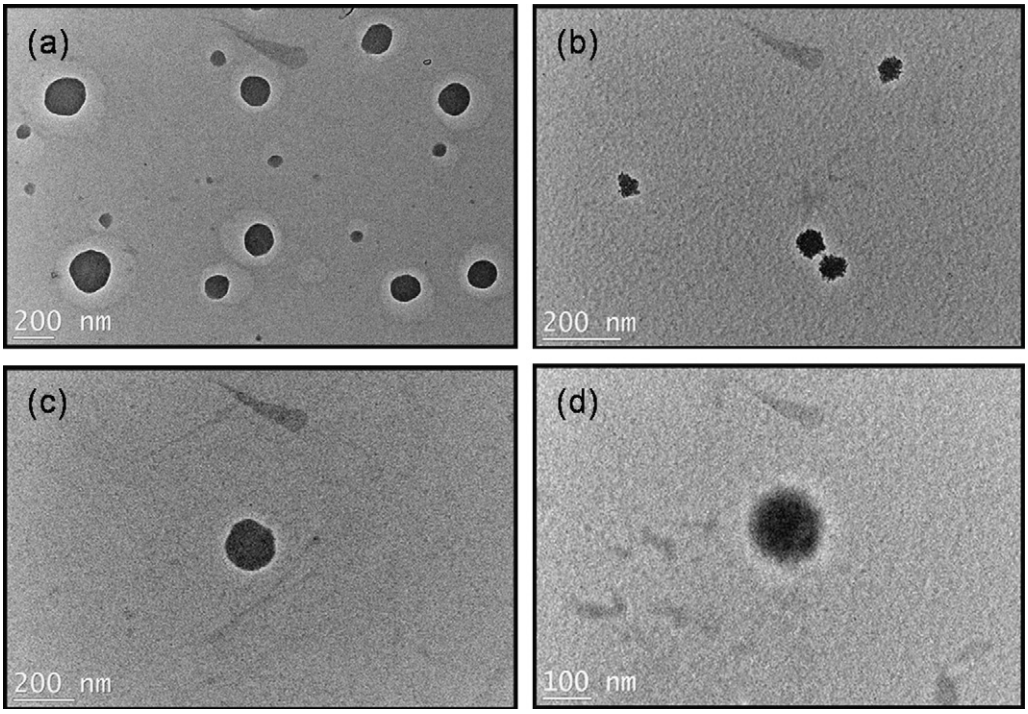

Fig. 3. Transmission electron microscopy images of silk fibroin nanoparticles prepared from *A. mylitta* (a), silk fibroin nanoparticles prepared from *B. mori* (b), a single silk fibroin nanoparticles prepared from *A. mylitta* (c), and a single silk fibroin nanoparticles prepared from *B. mori* (d).

3. Results and discussion

3.1. Particle size, surface charge, and stability of the nanoparticles

Nanoparticles of silk fibroin were prepared by desolvation method. The addition of desolvating agent reduces the available water to keep the fibroin molecules in water, resulting in reduction of hydrated fibroin chains. At certain point, the hydration becomes too low and silk fibroin protein precipitates in the form of nanoparticles (Weber et al., 2000; Azarmi et al., 2006). After freeze drying, a spongy mass was recovered with a yield of 80 ± 5%. The silk fibroin nanoparticles size determined by light scattering particle analyzer possess hydrodynamic diameter around 157 ± 4 nm (*A. mylitta*) with a polydispersity index of 0.020 compared to 177 ± 3 nm (*B. mori*) with a polydispersity index of 0.027. The silk fibroin nanoparticles were stable in cell culture medium containing 10% FBS (Table 1). The nanoparticles were found to show of 20 nm increase in diameter while immersed in serum containing medium possibly due to the adsorption of the serum proteins on to the surface of the silk nanoparticles. The particle size plays a significant role in the cellular and tissue uptake of the nanoparticles and in some cell lines only the sub-micron size particles are uptaken efficiently instead of the larger size microparticles (Lorenz et al., 2006).

The zeta potential is a concept used to describe the electrokinetics properties of a colloidal particle under the influence of an applied electric field (Azarmi et al., 2006). The presence of surface charge on the nanoparticles can cause them to show a higher absolute value of the zeta potential. The silk fibroin nanoparticles possess zeta potential in the range of −24 to −26 mV. The results suggest the presence of negative charges on the surface of the nanoparticles. The zeta potential of the particles decreased significantly to a lower value around −5 mV in the presence of serum (Table 1). This fact was explained by the shielding effect of serum proteins present on the particle surface and compensating for charge differences in deionized water and in serum containing deionized water.

The electrostatic repulsion of the nanoparticles prevents the polymer chains from uncontrolled agglomeration. After the formation of the silk protein nanoparticles, the surface of the nanoparticles possesses sufficient zeta potential to prevent further agglomeration of the particles. The surface charge and adsorbed molecules are possible issues affecting the size distributions of nanoparticles in the solvent. The silk nanoparticles were found to be stable in deionized water and also in cell culture medium containing serum over a longer period (Table 2).

3.2. FT-IR analysis of the nanoparticles

Protein shows characteristics vibration bands between 1630 and 1650 cm^{-1} for amide I (C=O stretching), 1540–1520 cm^{-1} for amide II (secondary N–H bending) and 1270–1230 cm^{-1} for amide III (C–N and N–H functionalities) in their FT-IR spectra. In addition, the positions of these bands indicate the conformations of the pro-

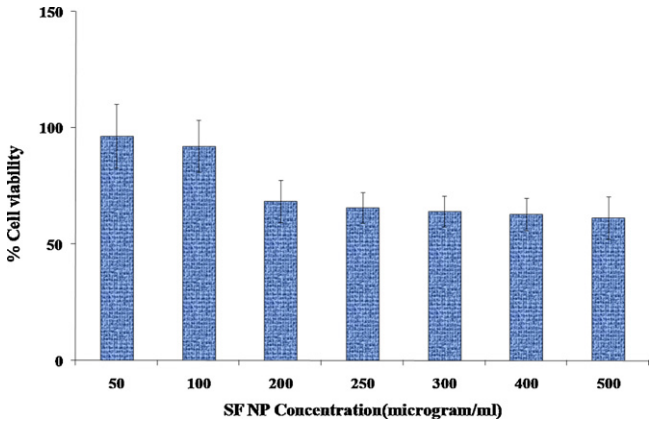

Fig. 4. Cytotoxicity profile of silk protein fibroin nanoparticles after 24 h incubation with murine L929 mouse fibroblast as determined by MTT assay. Percent viability of fibroblast is expressed relative to the control cells ($n = 6$).

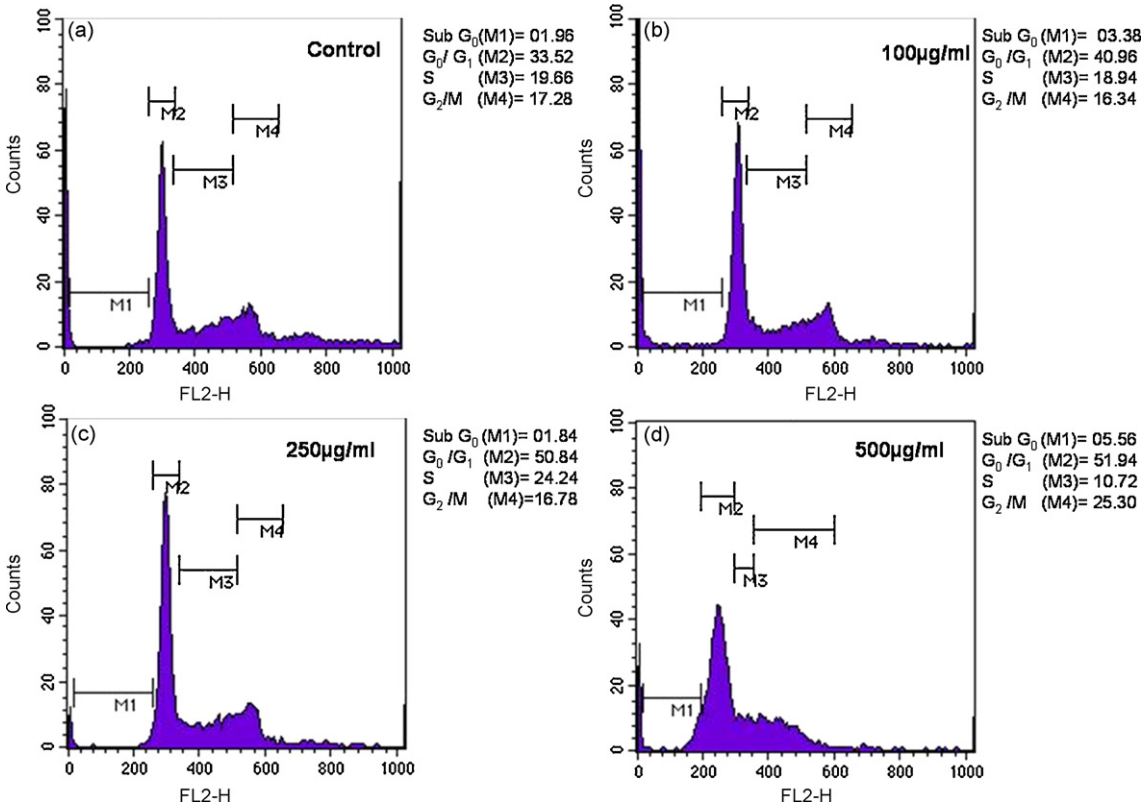

Fig. 5. Cell cycle analysis of L929 mouse fibroblast cells after 24 h incubation of silk protein fibroin nanoparticles with human fibroblast cells. Plots (a) cells incubated without nanoparticles, (b) cells incubated with 100 μg/ml nanoparticle suspensions, (c) cells incubated with 250 μg/ml of nanoparticle suspension, and (d) cells incubated with 500 μg/ml nanoparticle suspensions.

tein materials; 1650 cm^{-1} (random coil) and 1630 cm^{-1} (β-sheet) for amide I, 1540 cm^{-1} (random coil) and 1520 cm^{-1} (β-sheet) for amide II, and 1270 cm^{-1}(β-sheet) and 1230 cm^{-1} (random coil) for amide III. The FT-IR spectra of the silk fibroin nanoparticles from both mulberry and non-mulberry sources are shown in Fig. 1. The original silk fiber and freeze-dried fibroin show typical β-sheet and random coil structures, respectively (Tsukada et al., 1994). The regenerated fibroin film from dialyzed fibroin solution shows a very similar FT-IR spectrum to that of freeze-dried fibroin, also indicating random coil conformations (Gil et al., 2006; Um et al., 2001). The chemical shift of the absorption bands to 1632 cm^{-1} (amide I), 1521 cm^{-1} (amide II), 1233 cm^{-1} (amide III) attributed to the β-sheet structure in *B. mori* silk fibroin nanoparticles. The *A. mylitta* nanoparticles showed chemical shift of the absorption bands to 1673 cm^{-1} (amide I), 1517 cm^{-1} (amide II) and 1234 cm^{-1} (amide III) assigned to the β-sheet structures similar to those of the silk fibroin membranes after methanol treatment.

3.3. XRD measurement

XRD is generally used to study the crystalline structure of the material. Three types of crystalline structures are proposed for silk. The glandular state prior to crystallization is called the Silk I. Silk II is the spun silk state which consists of the β-sheet secondary structure and Silk III (an air/water assembled interfacial silk) is a helical structure (Kundu et al., 2008a,b). The main diffraction peaks of Silk I are present at around $2\theta = 12.2^\circ$ and 28.2°, while Silk II are present at about $2\theta = 18.9^\circ$ and 20.7°. Three distinct peaks were found in the X-ray diffractograms in the regions between 10° and 40°. Sharp peaks at $2\theta = 20.16^\circ$ denoting the Silk II conformation and at $2\theta = 24.16^\circ$ denoting the Silk I structure appeared in the XRD pattern of the nanoparticles made from *B. mori* protein as shown in Fig. 2. The XRD pattern of the nanoparticles made from *A. mylitta* protein showed three distinct peaks at $2\theta = 16.5^\circ$, 19.80° (both peaks denoting the Silk II conformation), and 23.59° (denoting the Silk I structure) signifying the conformational change from random coil state to β-sheet structure (Kweon et al., 2000; Mandal and Kundu, 2008).

3.4. TEM measurements

The TEM observation of the silk fibroin nanoparticles derived from liquid silk fibroin showed that they are spherical granules without apparent aggregation or adhesion (Fig. 3). Also, it should be noted that the particle size in TEM are relatively smaller than the particle size measured using DLS. This is due to the reason that, in DLS, the hydrodynamic size is measured and the particles are swollen, whereas, in electron microscopy studies, the hard sphere diameter is seen. The particles are solid and there is no evidence of them being hollow spheres (Liu et al., 2007). The fibroin nanoparticles prepared from *A. mylitta* were smoother and morphologically more spherical compared to the *B. mori* particles which were coarser and were not spherical in shape.

3.5. Cytotoxicity and cell cycle assays

The MTT assay is a common method for evaluating biomaterial toxicity based on the mitochondrial activity, which influences metabolic activity and cell viability (Mosmann, 1993; Gupta et al., 2004). To determine the toxicity profile of the newly synthesized silk protein fibroin nanoparticles, we conducted the standard MTT cytotoxicity assay with L929 fibroblast cells (Fig. 4). Cells incubated with silk protein fibroin nanoparticles at concentrations of 100 μg/ml remained almost 100% viable relative to control (equal

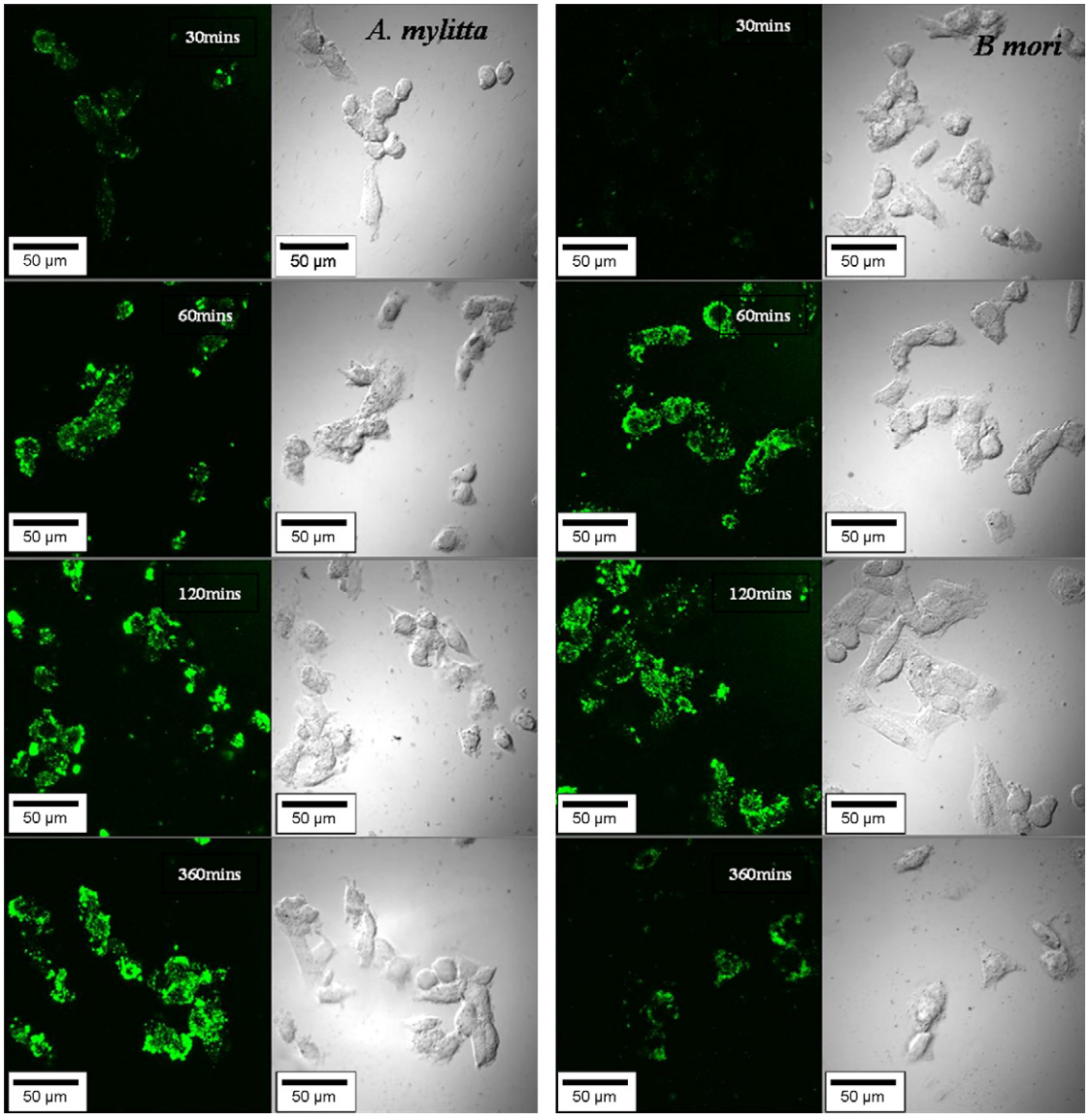

Fig. 6. Cellular uptake of nanoparticles prepared from regenerated fibroin protein solution obtained from non-mulberry tropical tasar silk gland and mulberry cocoons by murine squamous cell carcinoma cells (SCC7) after incubation for 30, 60, 120, and 360 min at 37 °C with 5% CO_2 atmosphere in a CO_2 incubator. (a) Detection of FITC labeled nanoparticles under fluorescence and (b) under bright field. Scale bar = 50 μm.

to 100%). However, at 200 μg/ml, the cell viability decreases but no further decrease in the cell viability was observed at higher concentrations (500 μg/ml). It is not clear what caused the apparent decrease in the viability at concentrations above 200 μg/ml, but since there is no dose dependent continuous decrease, it is hard to say that the nanoparticles caused severe cytotoxicity.

Live cell studies of cellular DNA content and cell cycle distribution are useful to detect variations of growth patterns to monitor apoptosis, to study tumor behavior and suppressor gene mechanism. Cell cycle analysis describes the progression of a cell through a cycle of division, a process resulting in cell growth and separation into two daughter cells. In Fig. 5, the gate cycle graphs are plotted after 24 h incubation of nanoparticles within the culture of L929 fibroblast cells. The gated percentage cells obtained in sub-G_0, G_0/G_1, S and G_2/M are shown. In the case of G_0/G_1 phases, the control culture showed approximately 33.52% cells compared to 40.96%, 50.84%, and 51.94% in the cases of 100, 250, and 500 μg/ml silk nanoparticles containing culture, respectively. In G_2/M phases, 17.28% was obtained in the control compared to 16.34%, 16.78%, and 25.30% in cultures containing 100, 250, and 500 μg/ml silk protein fibroin nanoparticles. 19.33% of cells were observed in the S phase of the control compared to 18.94%, 24.24%, and 10.72% in the cases of the cultures containing 100, 250, and 500 μg/ml silk protein fibroin nanoparticles, respectively. Therefore, the cells after 24 h culture with silk protein fibroin nanoparticles showed normal cell cycle distribution without any visible signs of cell cycle arrest. Overall, cytotoxicity and cell cycle assays indicated that silk fibroin nanoparticles are relatively non-toxic to the cells.

3.6. Cellular uptake of the nanoparticles

Labeling the nanoparticles with FITC (fluorescence isothiocyanate) had no statistically significant effect on the particle size and zeta potential (data not shown) of the silk nanoparticles. Cellular uptake of fluorescent labeled nanoparticles was demonstrated by confocal laser scanning microscopy (CLSM, Fig. 6) using murine squamous cell carcinoma cells (SCC7). We chose this cell line because of availability and its ability to form an adherent cell monolayer. For the initial 30 min, the uptake of the nanoparticles within the cells was minimal. After 1 h of incubation with the cells,

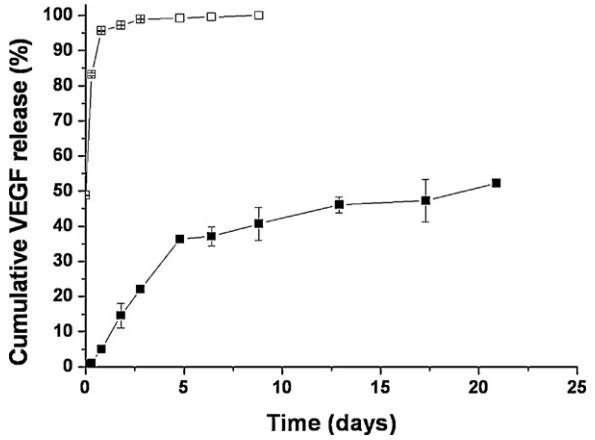

Fig. 7. Cumulative VEGF release ($n = 3$) at 37 °C from the silk fibroin nanoparticles obtained from tropical tasar silkworm, *A. mylitta* for the loading amount of 100 ng VEGF/5 mg of nanoparticles (■), and the control (100 ng VEGF alone) without the silk nanoparticles (□).

it was clearly visible that for both *A. mylitta* silk fibroin nanoparticles and *B. mori* silk fibroin nanoparticles, localization occurred in the perinuclear region. It is interesting to note that the cells remained viable during the course of this study and as such these silk nanoparticles did not confer any overt cytotoxicity (Gupta et al., 2004).

The nanoparticles internalization process into the cells can be considered as a binding (adsorbing) process followed by formation of vesicle and then the formed nanoparticle-containing vesicles are internalized by endocytosis (Foster et al., 2001; Osaka et al., 2009). At the initial time points, we observed the nanoparticles to be present mainly on the cell surface. Once the nanoparticles were endocytosed, they were found primarily in the cytoplasm around the nuclear membrane. We observed that a large fraction of the incubated nanoparticles were internalized by the cells and remained stable during vesicular transport in spite of their negative surface. The actual mechanism of internalization of our nanoparticles has yet to be determined.

3.7. *In vitro VEGF release*

VEGF release experiment was performed to evaluate the silk fibroin nanoparticles from tropical tasar silkworm, *A. mylitta* were used as potential therapeutic drug delivery system. VEGF was selected as a model growth factor for the *in vitro* release study as VEGF interacts with the net negatively charged silk fibroin nanoparticles (the isoelectric point of VEGF is pH 8.5) (Ferrara et al., 1992). Loading VEGF into the nanoparticles did not induce the aggregated complex formation. After loading VEGF into the silk nanoparticles by simple co-incubation at 4 °C, the total suspension solution was put into the release device without further washing or any other separation step. Thus, unbound, unloaded VEGF would have been released as an initial burst. However, no noticeable initial burst was observed at all. This implies an almost complete loading of VEGF into the nanoparticles at least in the present loading condition (100 ng of VEGF/5 mg of silk nanoparticles). The release of VEGF from the nanoparticles showed an initial linear profile without initial burst, releasing ~35% up to 5 days, followed by a more sustained release (~1% per day) after that (Fig. 7). In contrast, from the control system without the silk nanoparticles, VEGF was released completely within 3 days with a burst of ~90% during day 1. The developed nanoparticles may provide a ubiquitous drug carrier for the protein delivery due to their physiochemical properties, simple preparation methodologies and biocompatibility. Therefore, the silk nanoparticles can be used as an efficient sustained release system of VEGF, presumably based on the electrostatic interaction between VEGF and the silk nanoparticles.

4. Conclusion

The silk protein nanoparticles were around 150–170 nm in average diameter with narrow size distribution, negatively charged and stable in deionized water and serum containing culture medium. The conformation change of the regenerated silk fibroin nanoparticles were from the Silk I to Silk II structure as evident from the FT-IR and XRD analysis of the nanoparticles. *A. mylitta* nanoparticles were found to be finer and less coarse as compared to the *B. mori* particles. The silk fibroin nanoparticles were relatively non-toxic to the cells and showed normal cell cycle distribution without any visible signs of cell cycle arrest. Bioimaging analysis showed the accumulation of the silk nanoparticles by murine squamous cell carcinoma cells and they were present in the cytoplasm of the cells. The *in vitro* release of loaded VEGF in the nanoparticles showed a sustained release of over 3 weeks without initial burst. The silk fibroin protein possesses good biocompatibility, degradability and lot of active amino groups and tyrosine residues which favors the bioconjugation with other active molecules, pharmaceuticals and growth factors. The present investigation indicates the natural silk protein nanoparticles as carriers to deliver drugs to the target cells. The very simplified fabrication procedure of the silk fibroin nanoparticles may provide a novel tool to demonstrate the implications of the particles in cancer diagnostics and therapeutics.

Acknowledgements

This work was financially supported by Department of Biotechnology, Government of India, New Delhi and by the Korea-India R&D networking program (M60604000846-06A0400-84630) from Korea Foundation for International Cooperation of Science and Technology (KICOS), Ministry of Education, Science and Technology, Korea. This work was also partially supported by the World Class University (WCU) program at GIST through a grant provided by MEST of Korea (Project No. R31-2008-000-10026-0). SCK and JK are grateful to GIST for providing excellent hospitalities and facilities during their stay in Korea. Similarly GT and YHK express their gratitude to IIT Kharagpur for sincere hospitalities during their short stay in India.

References

Azarmi, S., Huang, Y., Chen, H., Mcquarrie, S., Abrams, D., Roa, W., Finlay, W.H., Miller, G.G., L'enberg, J., 2006. Optimization of a two step desolvation method for preparing gelatin nanoparticles and cell uptake studies in 143 B osteosarcoma cancer cells. J. Pharm. Pharmaceut. Sci. 9, 124–132.

Balthasar, S., Michaelis, K., Dinauer, N., von-Briesen, H., Kreuter, J., Langer, K., 2005. Preparation and characterization of antibody modified gelatin nanoparticles as drug carrier system for uptake in lymphocytes. Biomaterials 26, 2723–2732.

Cheema, S.K., Gobin, A.S., Rhea, R., Berestein, G.L., Newman, R.A., Mathur, A.B., 2007. Silk fibroin mediated delivery of liposomal emodin to breast cancer cells. Int. J. Pharm. 341, 221–229.

Chung, Y.I., Tae, G., Yuk, S.H., 2006. A facile method to prepare heparin-functionalized nanoparticles for controlled release of growth factors. Biomaterials 27, 2621–2626.

Datta, A., Ghosh, A.K., Kundu, S.C., 2001. Purification and characterization of fibroin protein from tropical Saturniid silkworm, *Antheraea mylitta*. Insect Biochem. Mol. Biol. 31, 1013–1018.

Ferrara, N., Houck, K., Jakeman, L., Leung, D.W., 1992. Molecular and biological properties of the vascular endothelial growth factor family of proteins. Endocr. Rev. 13, 18–32.

Foster, K.A., Yazdanian, M., Audus, K.L., 2001. Microparticulate uptake mechanisms of in-vitro cell culture models of the respiratory epithelium. J. Pharm. Pharmacol. 53, 57–66.

Gil, E.S., Frankowski, D.J., Bowman, M.K., Gozen, A.O., Hudson, S.M., Spontak, R.J., 2006. Silk fibroin membranes from solvent-crystallized silk fibroin/gelatin blends: effects of blend and solvent composition. Biomacromolecules 7, 728–735.

Gupta, A.K., Gupta, M., Yarwood, S.J., Curtis, A.S., 2004. Effect of cellular uptake of gelatin nanoparticles on adhesion, morphology and cytoskeleton organization of human fibroblast. J. Control. Release 95, 197–207.
Hofmann, S., Foo, C.T., Rossetti, F., Textor, M., Vunjak-Novakovic, G., Kaplan, D.L., Merkle, H.P., Meinel, L., 2006. Silk fibroin as an organic polymer for controlled drug delivery. J. Control. Release 111, 219–227.
Inoue, S., Tanaka, K., Arisaka, F., Kimura, S., Ohtomo, K., Mizuno, S., 2000. Silk fibroin of *B. mori* is secreted, assembling a high molecular mass elementary unit consisting of H-chain, L-chain, and P25, with a 6:6:1 molar ratio. J. Biol. Chem. 275, 40517–40528.
Jin, H.J., Fridrikh, S.V., Rutledge, G.C., Kaplan, D.L., 2002. Electrospinning *B. mori* silk with poly(ethylene oxide). Biomacromolecules 3, 1233–1239.
Jin, H.J., Park, J., Karageorgiou, V., Kim, U.J., Valluzzi, R., Cebe, P., Kaplan, D.L., 2005. Water stable silk films with reduced β sheet content. Adv. Funct. Mater. 15, 1241–1247.
Kaul, G., Amiji, M., 2005. Cellular interactions and *in vitro* DNA transfection studies with poly(ethylene glycol)-modified gelatin nanoparticles. J. Pharm. Sci. 94, 184–198.
Kim, U.J., Park, J., Li, C., Jin, H.J., Valluzzi, R., Kaplan, D.L., 2004. Structure and properties of silk hydrogels. Biomacromolecules 5, 786–792.
Kocbek, P., Obermajer, N., Cegnar, M., Kos, J., Krist, J., 2007. Targeting cancer cells using PLGA nanoparticles surface modified with monoclonal antibody. J. Control. Release 120, 18–26.
Kommareddy, S., Amiji, M., 2005. Preparation and evaluation of thiol-modified gelatin nanoparticles for intracellular DNA delivery in response to glutathione. Bioconjug. Chem. 16, 1423–1432.
Kundu, J., Patra, C., Kundu, S.C., 2008a. Design, fabrication and characterization of silk fibroin-HPMC-PEG blended films as vehicle for transmucosal delivery. Mater. Sci. Eng. C 28, 1376–1380.
Kundu, J., Dewan, M., Ghoshal, S., Kundu, S.C., 2008b. Mulberry non-engineered silk gland protein vis-à-vis silk cocoon protein engineered by silkworms as biomaterial matrices. J. Mater. Sci. Mater. Med. 19, 2679–2689.
Kweon, H., Um, I.C., Park, Y.H., 2000. Thermal behavior of regenerated Antheraea pernyi silk fibroin film treated with aqueous methanol. Polymer 41, 7361–7367.
Le, L.T., Walsh, S.M., Schweibert, E., Mao, H.Q., Guggino, W.B., August, J.T., 1999. Gene transfers by DNA–gelatin nanospheres. Arch. Biochem. Biophys. 361, 47–56.
Liu, Y.Y., Su, X., Tang, M.F., Kong, J., 2007. A facile method to prepare hydrophobic nanoparticle dispersions for controlled release. Macromol. Chem. Phys. 208, 415–422.
Liu, X.Y., Zhang, C.C., Xu, W.L., Ouyang, C., 2009. Controlled release of heparin from blended polyurethane and silk fibroin film. Mater. Lett. 63, 263–265.
Lorenz, M.R., Holzapfel, V., Musyanovych, A., Nothelfer, K., Walther, P., Frank, H., 2006. Uptake of functionalized, fluorescent-labeled polymeric particles in different cell lines and stem cells. Biomaterials 27, 2820–2828.
MaHam, A., Tang, Z., Wu, H., Wang, J., Lin, Y., 2009. Protein-based nanomedicine platforms for drug delivery. Small 5, 1706–1721.
Mandal, B.B., Kundu, S.C., 2008. Non-bioengineered high strength three-dimensional gland fibroin scaffolds from tropical non-mulberry silkworm for potential tissue engineering applications. Macromol. Biosci. 8, 807–818.
Mosmann, T., 1993. Rapid colorimetric assay for cellular growth and survival: application to proliferation and cytotoxic assay. J. Immunol. Methods 95, 55–63.
Muller, R.H., Mader, K., Gohla, S., 2000. Solid lipid nanoparticles (SLN) for controlled drug delivery—review of the state of the art. Eur. J. Pharm. Biopharm. 50, 161–177.
Nazarov, R., Jin, H.J., Kaplan, D.L., 2004. Porous 3D scaffolds from regenerated silk fibroin. Biomacromolecules 5, 718–726.
Osaka, T., Nakanishi, T., Shanmugam, S., Takahama, S., Zhang, H., 2009. Effect of surface charge of magnetite nanoparticles on their internalization into breast cancer and umbilical vein endothelial cells. Colloids Surf. B 71, 325–330.
Soppimath, S.K., Aminabhavi, T.M., Kulkarni, A.R., Rudzinski, W.E., 2002. Biodegradable polymeric nanoparticles as drug delivery devices. J. Control. Release 70, 1–20.
Svenson, S., Tomalia, D.A., 2005. Dendrimers in biomedical applications—reflection on the field. Adv. Drug Deliv. Rev. 57, 2106–2129.
Tanaka, K., Inoue, S., Mizuno, S., 1999. Hydrophobic interaction of P25, containing Asn-linked oligosaccharide chains, with the H–L complex of silk fibroin produced by *B. mori*. Insect Biochem. Mol. Biol. 29, 269–276.
Torchilin, V.P., 2004. Targeted polymeric micelles for delivery of poorly soluble drugs. Cell Mol. Life Sci. 61, 2549–2559.
Tsukada, M., Gotoh, Y., Nagura, M., Minoura, N., Kasai, N., Freddi, G., 1994. Structural changes of silk fibroin membranes induced by immersion in methanol aqueous solutions. J. Polym. Sci. B: Polym. Phys. 32, 961–968.
Uebersax, L., Mattotti, M., Papaloïzos, M., Merkle, H.P., Gander, B., Meinel, L., 2007. Silk fibroin matrices for the controlled release of nerve growth factor (NGF). Biomaterials 28, 4449–4460.
Um, I.C., Kweon, H.Y., Park, Y.H., Hudson, S., 2001. Structural characteristics and properties of the regenerated silk fibroin prepared from formic acid. Int. J. Biol. Macromol. 29, 91–97.
Wang, X., Wenk, E., Matsumoto, A., Meinel, L., Li, C., Kaplan, D.L., 2007. Silk microspheres for encapsulation and controlled release. J. Control. Release 117, 360–370.
Weber, C., Coester, C., Kreuter, J., Langer, K., 2000. Desolvation process and surface characterization of protein nanoparticles. Int. J. Pharm. 194, 91–102.
Won, Y.W., Kim, Y.H., 2008. Recombinant human gelatin nanoparticles as a protein drug carrier. J. Control. Release 127, 154–161.
Xu, W., Ke, G., Peng, X., 2006. Studies on the effects of the enzymatic treatment on silk fine powder. J. Appl. Polym. Sci. 101, 2967–2971.
Zhao, J., Wu, J., 2006. Preparation and characterization of the fluorescent chitosan nanoparticle probe. Chinese J. Anal. Chem. 34, 1555–1559.